

Impact of surface modification of green algal biomass by phosphorylation on the removal of copper(II) ions from water

Zakaria AL-QODAH^{1,2}, Mohammad AL-SHANNAG^{3,*}, Abdulaziz AMRO⁴,
Eman ASSIREY⁴, Mustafa BOB⁵, Khalid BANI-MELHEM⁶, Malek ALKASRAWI⁷

¹Department of Chemical Engineering, Taibah University, Medina, Saudi Arabia

²Department of Chemical Engineering, Al-Balqa Applied University, Amman, Jordan

³Department of Chemical Engineering, School of Engineering, University of Jordan, Amman, Jordan

⁴Department of Chemistry, Taibah University, Medina, Saudi Arabia

⁵Department of Civil Engineering, Taibah University, Medina, Saudi Arabia

⁶Department of Water Management and Environment, Faculty of Natural Resources and Environment,
Hashemite University, Al-Zarqa, Jordan

⁷Department of Paper Engineering, University of Wisconsin, Stevens Point, WI, USA

Received: 18.05.2016

Accepted/Published Online: 01.09.2016

Final Version: 19.04.2017

Abstract: A series of batch lab-scale experiments were performed to investigate the performance of dead phosphorylated algal biomass of *Spirogyra* species for the bioadsorption of Cu^{+2} ions from aqueous solutions. FT-IR and SEM analyses were performed to characterize the phosphorylated and raw algae. The SEM analysis indicated that the phosphorus content increases by about 5 times. The isotherm equilibrium data indicated that phosphorylation enhances the removal of Cu^{+2} from water by about 20%. The experimental isotherms fit well to Langmuir models with R^2 values close to 0.99. Adsorption kinetic study was conducted to investigate the effect of initial Cu^{+2} concentrations, pH, and adsorbent dose on the loading capacity of algal biomass. The optimum pH for the process was around 6 and the corresponding maximum loading capacity was 65 mg/g. The pseudo second-order kinetics successfully modeled the kinetic results with R^2 values closed to 0.99. The thermodynamic results indicated that the bioadsorption process is endothermic and spontaneous at initial Cu^{+2} concentrations lower than 100 mg/L. The results were promising and encourage the design of a continuous process using algal biomass to remediate water polluted with heavy metals.

Key words: Copper removal, algae, *Spirogyra*, adsorption isotherms, bioadsorption, adsorption kinetics, phosphorylation

1. Introduction

The remarkable increase of industrial processes and human activities intensified environmental contamination and pollution problems¹⁻³. The accumulation of heavy metals in the environment leads to many health problems on one hand^{4,5} and to the deterioration of many ecosystems on the other hand⁶. As a consequence, there are ever increasing legislative standards in most countries that impose treatment processes to reduce heavy metal concentrations or to recover them where feasible. The metals ions of primary concern according to the World Health Organization are those of aluminum, cadmium, chromium, cobalt, copper, iron, manganese, mercury, lead, arsenic, and nickel.^{6,7} Copper is considered as one of the most toxic and widely used materials

*Correspondence: mohammad_al.shannag@hotmail.com

since it is involved in a variety of industries including electronic and electrical devices and equipment, metal plating, mining, ceramic glazing, glass coloring, and many others. These industries and others discharge a huge amount of wastewater contaminated with a significant amount of copper.^{4,5,8-10} Notably, Cu^{+2} ions are known as persistent, nondegradable, bioaccumulative, and toxic chemical species. This ion has many adverse effects on the environment and human health. In humans, Cu^{+2} concentrations above 0.05 mg/L can cause serious medical problems including severe mucosal irritation, anemia, stomach intestinal distress, central nervous problems followed by depression, and kidney damage upon prolonged exposure.¹¹⁻¹⁶ Accordingly, the strict environmental regulations have made it compulsory to search for new efficient and environmentally friendly processes for removal of metal ions from wastewater to reduce their concentrations below the maximum allowable limits.^{1,5,17}

Many processes for Cu^{+2} ion removal have been applied in the last two decades. These include evaporative recovery, ion exchange, reverse osmosis, electrochemical treatment, and adsorption.¹¹ However, the application of most of these processes is often limited due to technical or economic constraints.^{10,18} Among these processes, adsorption is highly recommended because it is proven as a simple, economical, effective, and environmental friendly process.¹⁹⁻²² Among various adsorbents used, activated carbon is considered as the most efficient material used due to several important properties that enhance the adsorption process.²³ These properties include the high surface area, environmental friendliness, and ease of operation.²⁴ However, activated carbon is economically not feasible. This drawback has led to the search for suitable cheap and efficient adsorbents.²⁵

Recently, several types of bioadsorbents including some agricultural wastes, living and nonliving fungi, algae, and bacteria have been used as efficient and low-cost alternatives.^{1,25-29} However, the use of nonliving cells as metal binding bioadsorbents has been gaining advantages becoming more attractive and practical than living cells. This is because of the fact that living cells will be deactivated by toxic heavy metals ions, resulting in cell death.³⁰ Moreover, living cells usually grow in a fermentation medium that contains nutrients. These nutrients increase both biological oxygen demand and chemical oxygen demand in the effluent.³¹ In addition, when using dead cells, both the adsorbed metal ions and the biomass used can be easily recovered and regenerated using suitable chemical and physical processes. This will lead to repeated use of the biomass and better process economy.³²

Algae are cheap and available filamentous microorganisms obtained from marine or fresh water. They have been successfully used as bioadsorbents for heavy metal ions from industrial wastewater.³²⁻³⁴ However, it was clear from previous studies that the adsorption capacity of raw algae is not high. This implies that green algae need some pretreatment processes including surface modification by the introduction of some active functional groups in order to enhance the adsorption capacity.

Hassan Khani et al³⁵ used acids and CaCl_2 to treat marine algae *Cystoseira indica* for the adsorption of uranium from aqueous solutions. They found that the maximum uranium adsorption capacity on the Ca-pretreated, protonated, and nonpretreated *C. indica* algae predicted by Langmuir isotherm at pH 4 and 30 °C was 454.5, 322.58, and 224.67 mg/g, respectively. Parameswari et al³⁶ performed a pretreatment of blue green algal biomasses to investigate the impact on the bioadsorption capacity of Cr(VI) and Ni(II) under single and binary metal conditions. They used physical treatments such as autoclaving and chemical treatments using sodium hydroxide and acetic acid. They reported that under the single metal condition, all the pretreated biomass had increased biosorption of Cr(VI) and Ni(II) in comparison with live biomass by 27.90%.

Recently, Ahmady-Asbchin and Mohammadi³⁷ studied the bioadsorption properties of Cu^{+2} by a

pretreated biomass of marine algae *Fucus vesiculosus*. They reported that the adsorption equilibrium data were best fitted by the Langmuir isotherm model. In a more recent study, Mikati et al.³⁸ used HCl and citric acid to modify the surface of *Chaetophora elegans* algae in order to improve the methylene blue adsorption. Soleymani et al.³⁹ used magnesium nitrate to modify the surface of brown algae for the bioadsorption of cobalt(II).

Notably, large quantities of algae and algal wastes are annually produced, and these quantities can be reused in many processes.⁴⁰ Moreover, it is evident from the above survey that algae represent a potential adsorbent for heavy metals after pretreatment with a suitable reagent. However, very limited studies are available in the literature concerning the pretreatment of algae to enhance the adsorption capacity. In addition, the phosphorylation of algae has never been investigated before. For this reason, the primary objective of this investigation is to perform a phosphorylation process on dead algae cells in order for them to be used as a bioadsorbent for copper ion Cu^{+2} . Several kinetic and isotherm models will be applied to fit the experimental data. The effects of different operational parameters such as temperature, pH, adsorbent mass, and Cu^{+2} initial concentration will be investigated.

1.1. Adsorption isotherm models

Adsorption isotherms models are usually used to further explore the adsorption mechanism. These models indicate the distribution of the adsorbate molecules between the liquid phase and a unit mass of the adsorbent solid phase at equilibrium state. Two of the most common sorption models were used to fit the experimental data. These models are the Langmuir and Freundlich isotherm equations.^{1,5} The Langmuir model assumes the presence of homogeneously distributed active sites on the adsorbent surface. The finite active site pattern leads to the formation of a monolayer of the adsorbate molecules on the adsorbent surface. This model, shown in the following equation, has successfully described many metal ions' bioadsorption onto bioadsorbents:

$$Q_e = \frac{bQ_m C_e}{1 + bC_e}, \quad (1)$$

where C_e is the equilibrium concentration of the Cu^{+2} in mg/L, Q_m is the Langmuir constant related to the saturation adsorption capacity in mg/g, and b , in L/mg, is a constant related to the affinity between the adsorbent and the adsorbate or the sorption equilibrium constant. The linear form of the Langmuir model can be expressed as:

$$\frac{1}{Q_e} = \frac{1}{Q_m} + \frac{1}{bQ_m C_e}. \quad (2)$$

The values of parameters Q_m and b can be determined by plotting $1/Q_e$ versus $1/C_e$ to obtain a straight line of slope equal to $1/Q_m$ and $1/bQ_m$ as an intercept.

In addition, an essential feature of the Langmuir isotherm may be expressed in terms of a unitless equilibrium parameter R_L , which is a constant referred to as the separation factor or equilibrium parameter:⁴¹

$$R_L = \frac{1}{1 + (1 + bC_o)}, \quad (3)$$

where C_o is the initial concentration in mg/L. The R_L value indicates the adsorption nature to be unfavorable if $R_L > 1$, linear if $R_L = 1$, and favorable if $0 < R_L < 1$.

The second model used to describe the adsorption of metal ions is the Freundlich model. In contrast to the Langmuir model, this model assumes a heterogeneous solid surface with nonequivalent binding sites. In this case, an initial surface for adsorption of some ions takes place followed by a condensation of more ions as a result of extremely strong ion-ion interaction. This model is described by:

$$Q_e = K_f C_e^{1/n}, \quad (4)$$

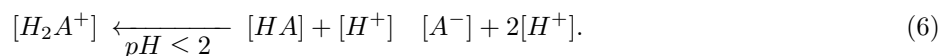
where K_F in $(L/mg)^{1/n}$ and n (unitless) are Freundlich constants. K_F represents the maximum adsorption capacity and n gives an indication of the adsorption intensity or how favorable the adsorption process is.^{1,5,11} The linear form of this model takes the following form:

$$\log Q_e = \log K_F + (1/n) \log C_e. \quad (5)$$

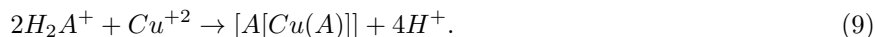
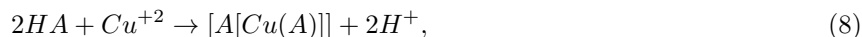
To evaluate Freundlich constants K_F and n , a plot of $\log Q_e$ versus $\log C_e$ will give a straight line of a slope equal to $1/n$ and $\log K_f$ as an intercept.

1.2. Kinetic modeling

The algal cell surface is characterized by its complex nature as it contains different active functional groups including mainly carboxyl and hydroxyl groups. These functional groups and consequently their availability to bind with metals such as Cu^{+2} are strongly affected by the pH value of the solution.^{40,42} Mukhopadhyay et al.⁴ proposed a reaction model of the algal surface functional groups with H^+ ions at different pH values to produce several surface active sites that participate in the bioadsorption process. This model equation is expressed by:



Eq. (6) indicates that there are three different species of active sites on the algal surface depending on the pH value. These sites are named as A^- , HA , and H_2A . The reactions of these species with Cu^{+2} can be described by the following chemical equations:



It is clear that Eqs. (7) through (9) represent reactions or bioadsorption processes between divalent Cu^{+2} ions with three different ligands. However, these reactions cannot take place at the same time since one ligand is predominant at a certain pH. In addition, most studies have indicated that the optimum pH for the bioadsorption of Cu^{+2} is in the range of 5 to 6 since $Cu(OH)_2$ starts to precipitates beyond a pH value of 6.^{4,28} Accordingly, most of the active sites in the optimum pH range will be in the form of A^- represented by Eq. (7). For this reason, the chemical reaction represented by Eq. (7) will be considered in this investigation. The rate expression for this reaction could be described by the second-order rate equation.⁴³ However, this model will be modified to the pseudo second-order rate expression, shown in the following equations, since the adsorbed

amount of Cu^{+2} ions at time t and at equilibrium will be used in the present research rather than the solution concentration:

$$\frac{dQ_t}{dt} = k(Q_e - Q_t)^2, \quad (10)$$

where Q_e represents the number of active sites occupied by Cu^{+2} ions at equilibrium or is the amount of Cu^{+2} ions adsorbed per unit mass of adsorbent at equilibrium, mg/g, and Q_t represents the number of active sites occupied by Cu^{+2} ions at any time t or the amount of Cu^{+2} ions adsorbed per unit mass of adsorbent, mg/g, at any time. In addition, k is the pseudo-second order constant, g/(mg h). Eq. (10) can be rearranged in the following form:

$$\frac{dQ_t}{(Q_e - Q_t)^2} = k dt, \quad (11)$$

and integrated between the following boundary conditions:

$Q_t = 0$ at $t = 0$ and $Q_t = Q_t$ at $t = t$, to give:

$$\frac{t}{Q_t} = \frac{1}{kQ_e^2} + \frac{t}{Q_e}. \quad (12)$$

The value of k can be determined by plotting t/Q_t versus t to obtain a straight line with a slope of $1/Q_e$ and intercept of $1/kQ_e^2$, which is defined as the initial rate in mg/(g h) as t approaches zero.

1.3. Thermodynamic modeling

In the present research, the thermodynamic parameters for the bioadsorption process, the standard enthalpy (ΔH°) in J/mol, the standard free energy (ΔG°) in J/mol, and the standard entropy (ΔS°) in J/(mol K), were calculated using the following equations:⁴⁴

$$\ln K_d = \frac{\Delta S^\circ}{R} - \frac{\Delta H^\circ}{RT}, \quad (13)$$

where $R = 8.314$ J/(mol K) is the universal gas constant, T is the absolute solution temperature in K, and K_d is the distribution coefficient, which is given by:

$$K_d = \frac{C_{Ae}}{C_e}, \quad (14)$$

where C_{Ae} , in mg/L, is the amount of Cu^{+2} ions adsorbed on algae at equilibrium and C_e , in mg/L, is the Cu^{+2} ions' equilibrium concentration. A plot of $\ln K_d$ versus $1/T$ will give a straight line of a slope equal to $-\Delta H^\circ/R$ and an intercept of $\Delta S^\circ/R$. On the other hand, ΔG° can be calculated using:

$$\Delta G^\circ = -RT \ln K_d. \quad (15)$$

2. Results and discussion

2.1. Algal biomass characterization

Fourier transform infrared (FT-IR) spectroscopy is an important analytical method used in this investigation to predict the functional groups that exist in the algae *Spirogyra* in order to explain the affinity toward Cu^{+2} ions.

Figure 1a depicts the FT-IR spectrum of a sample of these green algae and shows the major functional groups. As shown in Figure 1a, the strong absorption bands at 3371 and 3408 cm^{-1} in the spectra are attributed to the intramolecular hydrogen bonded O-H stretching vibration and to the N-H group. In addition, it indicates the presence of carbonyl groups, C=O, an amino group, N-H, and hydroxyl groups, O-H. Moreover, bands at 1155 and 895 cm^{-1} are characteristic of ester groups. On the other hand, the absorption bands of 1246 cm^{-1} and 1258 cm^{-1} are due to sulfate ester groups, S=O. These bonds increase the ability of green algae to adsorb metal ions from water since these groups are rich in electron lone pairs as in the case of Lewis bases. These

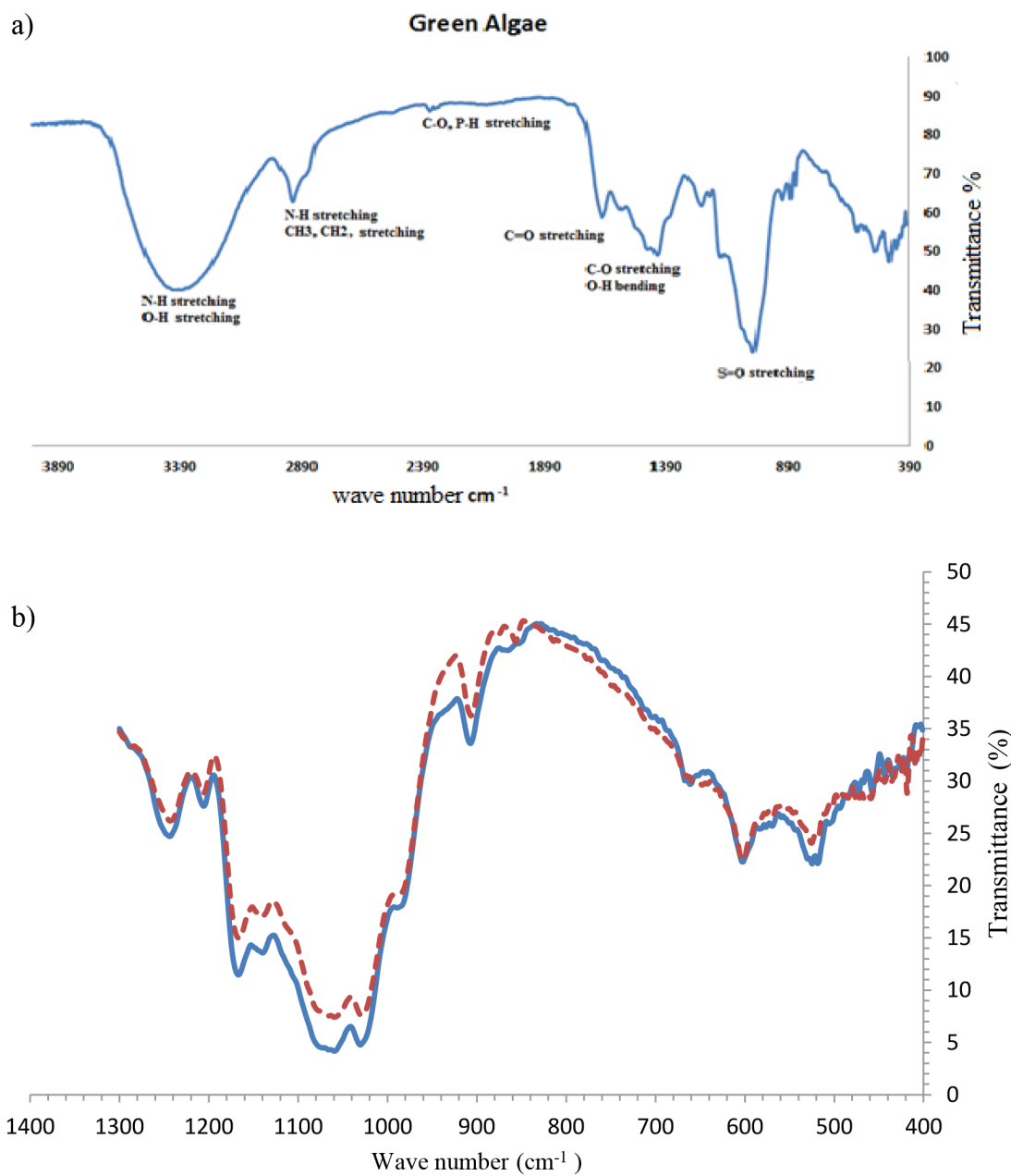


Figure 1. FT-IR of green algae: a) before phosphorylation; b) a comparison between FT-IR bands of green algae before (dashed line) and after (solid line) phosphorylation.

groups indicate the presence of polysaccharides, amino acids, esters, and pectin molecules in the algal structure as confirmed by Kannan.⁴² The presence of molecules and their characteristic functional groups explain the ability of algae to act as a Lewis base and easily coordinate and adsorb heavy metal ions such as copper(II).

The energy dispersive (EDS) X-ray in Figure 1b shows that the FT-IR window from 400 to 1300 cm^{-1} clearly indicates the changes of green algae spectra after phosphorylation. Green algae have a phosphate group before phosphorylation, as shown in Figure 1. However, the phosphorylation step increases the phosphate groups in the algal structure. The shoulders at 504 and 531 cm^{-1} of the P-O stretching become sharper after phosphorylation.⁴² Furthermore, the shoulder at 987 cm^{-1} becomes sharper. C-O-P stretching in phosphate esters at 1064 cm^{-1} also shows a small shoulder. Finally, sharper peaks are present at 1240 cm^{-1} as a result of P=O asymmetric stretching.⁴⁵ The EDS results for algae before and after phosphorylation are shown in Table 1. It is evident from Table 1 that phosphorus weight and atom percent increase from 0.46 to 2.17 and from 0.21% to 1.01%, respectively. This increase in the phosphorus content, which is about 5 times, is expected to enhance metal coupling and thereby the bioadsorption process.

Table 1. Mass composition EDS analysis results of *Spirogyra* green algae before and after phosphorylation.

Element	Before phosphorylation		After phosphorylation	
	Weight %	Atoms %	Weight %	Atoms %
C	34.30	40.64	30.89	37.19
N	9.19	9.33	10.04	10.37
O	55.74	49.58	56.89	51.42
F	0.32	0.24	0.00	0.00
P	0.46	0.21	2.17	1.01
Total	100.00	100.00	100.00	100.00

Figures 2a and 2b show the scanning electron microphotograph of *Spirogyra* green algae with two magnifications, 250 \times and 1000 \times . It is clear from Figures 2a and 2b that the morphology of green algae reflects a huge surface area. This large surface area increases the probability of higher metal ions being removed from wastewater.

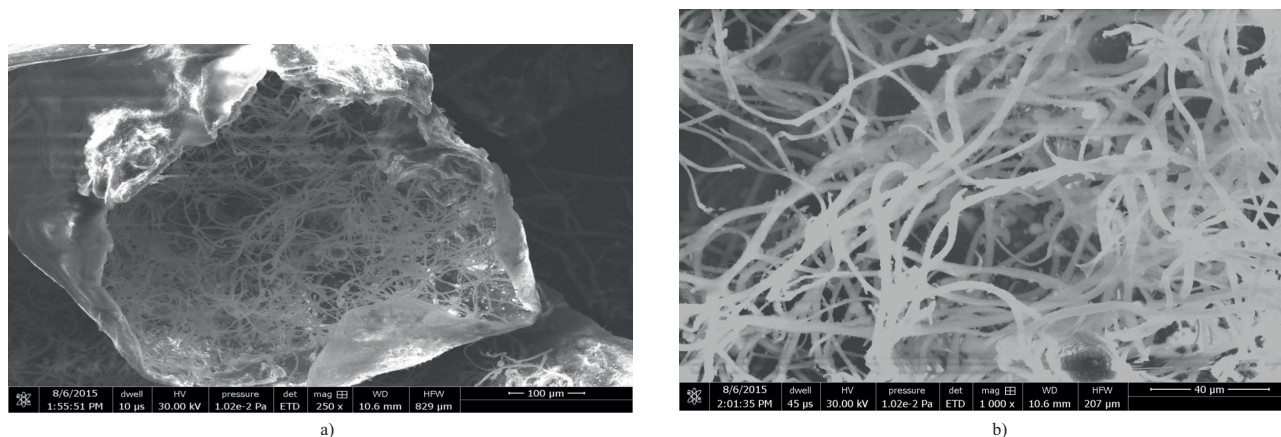


Figure 2. SEM image of *Spirogyra* green algae: a) 250 \times , b) 1000 \times .

2.2. Adsorption isotherms

The results of adsorption isotherm experiments usually have a significant impact on the feasibility of any adsorption research. These results usually show how much of the adsorbate ions or molecules are transferred from the solution to the adsorbent at equilibrium conditions. In addition, the results indicate the effect of adsorbate equilibrium concentration on the loading capacity of the adsorbent at different temperatures. Figure 3 depicts the adsorption isotherms of Cu^{+2} ions onto both phosphorylated and raw algal biomass at three different temperatures of 30, 40, and 50 °C. It is clear from Figure 3 that the loading capacity, Q_e , of the algal

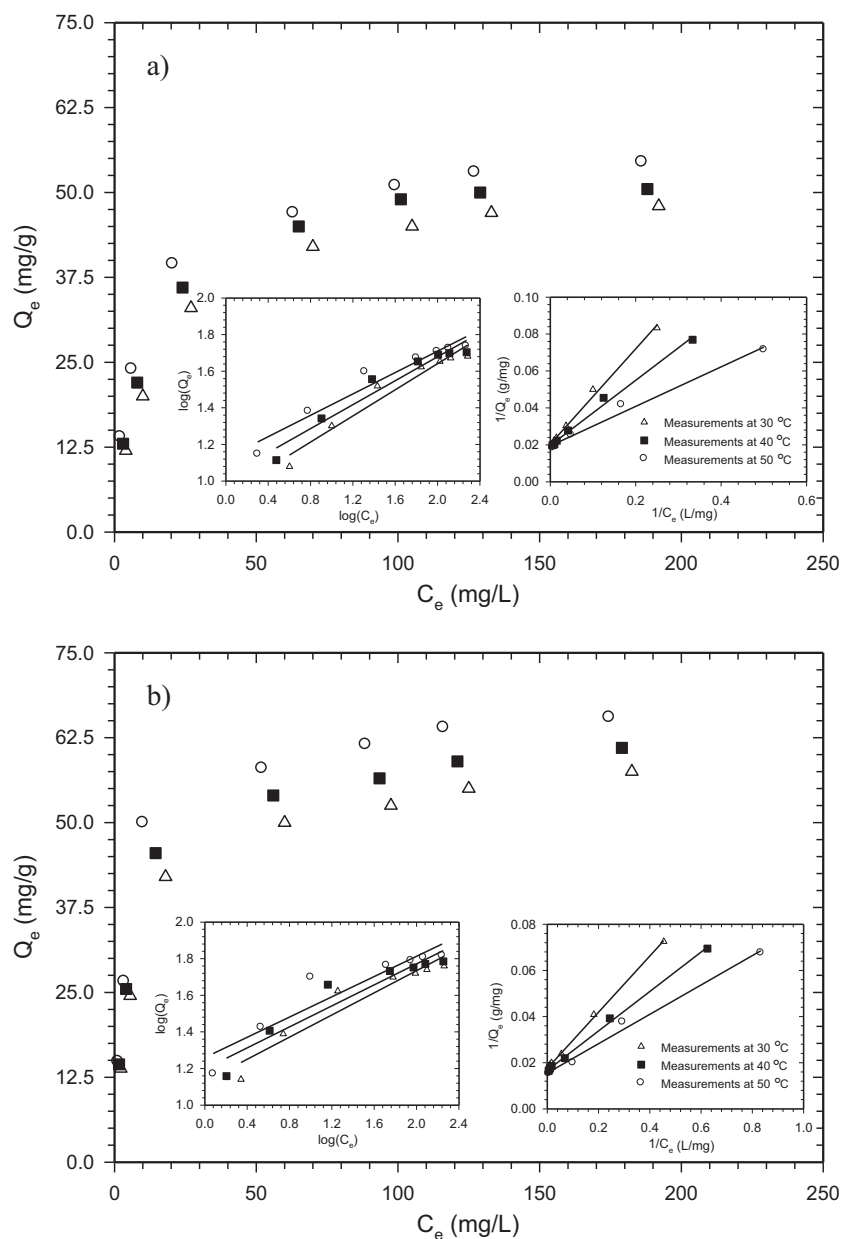


Figure 3. Adsorption isotherms of Cu^{+2} ions onto algal biomass with particles of 300 μm in diameter at three different temperatures, mixing speed of 150 rpm, and 24 h of incubation time: a) before phosphorylation and b) after phosphorylation.

mass increases as the equilibrium concentration increases until it reaches a pseudo steady-state value depending on the operating temperature's increase. In addition, the phosphorylated algae show higher adsorption capacity at all temperature compared to unphosphorylated algae. When the initial Cu^{+2} ions' concentration was 240 mg/L, the pseudo steady-state values of Q_e for the phosphorylated algae were 57.5, 61.0, and 65.5 mg/L and those of the unphosphorylated algae were 48, 50.5, and 54.5 mg/L, corresponding to 30, 40, and 50 °C, respectively. These values indicate two main results: the first result is that increasing the temperature will improve the loading capacity of the algal biomass. This is in agreement with the findings of Bishnoi et al.⁷ However, this improvement is not large and it reaches about 14% as the temperature increases from 30 to 50 °C. This increase in the loading capacity is attributed mainly to the effect of temperature on the solution viscosity and to the ions' kinetic energy. It is known that the viscosity of a solution decreases and the kinetic energy of the ions increases as the temperature increases. These effects, in addition to the possible enlargement of the pore size as temperature increases, will enhance the intraparticle diffusion of the Cu^{+2} ions and their contact time with the active sites.^{1,28} The second important result is that phosphorylation of the algal biomass enhances the adsorption capacity. The enhancement percentages were 20%, 21%, and 22% corresponding to 30, 40, and 50 °C, respectively. This indicates the feasibility of the phosphorylation process for bioadsorbents to increase their adsorption capacity. Moreover, it is evident from Figure 3 that for all samples and at all temperatures the loading capacity of the algal cells increases at a high rate at a relatively low equilibrium concentration. On the other hand, the rate at relatively high equilibrium concentrations continuously decreases until it becomes about zero when reaching the maximum loading capacity (Q_m). This behavior of the adsorption process is favorable since it indicates high affinity between the algal biomass and Cu^{+2} ions.

The values of the separation parameter R_L for the adsorption of Cu^{+2} were 0.453, 0.216, and 0.171, corresponding to initial concentrations of 50, 150, and 250 mg/L, respectively. These values fall in the preferred region (i.e. $0 < R_L < 1$). The results thus certify that algal biomass is a good adsorbent for the removal of Cu^{+2} heavy metal ions in aqueous solutions.

Two adsorption isotherm models were examined to fit the experimental results. These are the Langmuir and Freundlich isotherm models. The inserts in Figure 3 show the linear plots of these isotherm models. The values of the model parameters and the values of the correlation coefficient, R^2 , are shown in Table 2. It is evident from Table 2 that the Langmuir isotherm fits the adsorption data better than the Freundlich model, as indicated by R^2 values. This behavior indicates that the adsorbed Cu^{+2} ions form a monolayer coverage on the algal biomass outer surface. In addition, this adsorption has a homogeneous nature or equal activation energy for each adsorbed molecule. In addition, Table 2 depicts that the values of the maximum monolayer loading capacity of the phosphorylated algae, Q_m , predicted by the Langmuir model are about 8% higher than the experimental results. For example, the experimental value of the maximum loading capacity at 30 °C and 240 mg/L Cu^{+2} ions is 57.5 mg/g, whereas that predicted by the model is 57.14 mg/g. However, the present experimental values of Q_e are 50% higher than those reported in the study of Bishnoi et al.⁷ and comparable to those of Al-Rub et al.⁵ It is clear from Table 2 that the phosphorylated algae have higher values of Q_m than the unphosphorylated samples. For example, at 50 °C, Q_m of the phosphorylated algae and the unphosphorylated algae is about 64.31 and 51.58 mg/g, respectively. The difference is about 26%, which is significant at this temperature. Based on these results, the rest of the experiments concerning the kinetics and desorption were carried out using phosphorylated algal biomass.

Table 2. Langmuir and Freundlich isotherm models' parameters and the corresponding values of the squared correlation coefficient, R^2 .

Isotherms	Temperature (K)	Constants		R^2
Langmuir $\frac{1}{Q_e} = \frac{1}{Q_m} + \frac{1}{bQ_m C_e}$	Before phosphorylation			
	303	Q_m (mg/g) 49.11	b (L/mg) 0.079	0.9940
	313	50.78	0.112	0.9928
	323	51.58	0.181	0.9800
	After phosphorylation			
	303	Q_m (mg/g) 57.14	b (L/mg) 0.144	0.9989
	313	60.24	0.194	0.9981
	323	64.31	0.244	0.9927
	Freundlich $\log Q_e = \log K_F + (1/n) \log C_e$	Before phosphorylation		
303		$K_F ((L/mg)^{1/n})$ 8.44	n 2.80	R^2 0.9496
313		10.57	3.05	0.9440
323		13.34	3.42	0.9448
After phosphorylation				
303		$K_F ((L/mg)^{1/n})$ 13.56	n 3.30	R^2 0.915
313		15.78	3.48	0.9054
323		18.18	3.61	0.8779

2.3. Adsorption kinetics

A better understanding of the effect of operational parameters on the rate of metal uptake by the adsorbent is of primary importance for the successful development of adsorption-based water purification systems. This will help to determine the time needed to establish equilibration with maximum uptake. In addition, it provides a method to understand the kinetics of the sorption process. For this reason, the impact of several operational parameters such as adsorbent mass, pH, temperature, and adsorbent dose on the adsorption characteristics of Cu^{+2} ions onto the algal biomass are investigated in the present research.

2.3.1. Effect of contact time and initial concentration of Cu^{+2}

The effect of initial concentration on the adsorption of Cu^{+2} onto algal biomass was studied using three values of 50, 100, and 150 mg/L. Each batch adsorption process continued for 150 min. The variations of the adsorption capacity and removal efficiency with time at different initial concentrations are shown in Figure 4. It is clear from Figure 4a that the rate of Cu^{+2} ion uptake by the algal biomass was relatively high in the first 20 min for the three concentrations. This behavior indicates that there is a strong interaction between Cu^{+2} and algal biomass. The quantity of Cu^{+2} adsorbed, Q_t , increases as the contact time increases with a gradual decreasing rate until it reaches a plateau after 120 to 180 min. This plateau or pseudo steady-state value is known as the equilibrium loading capacity, Q_e . This behavior is typical for all initial concentrations. It should be noted that when this pseudo steady state is attained the Cu^{+2} ions in the solutions are found in a state of dynamic equilibrium with those adsorbed Cu^{+2} ions. In addition, the figure shows that both the rate of adsorption and the equilibrium loading capacity, Q_e , increase as the initial metal ions' concentration increases. This is attributed to the concentration gradient between the solution and the adsorbent surface at the initial metal ion concentrations. For initial concentrations of 50, 100, and 150 mg/L, the equilibrium loading capacity, Q_e , was 38.0, 49.1, and 52.5 mg/L, respectively, at a temperature of 30 °C, pH of 5.6, and mixing speed of 300 rpm. As can be seen in Figure 4b, 80% of the adsorbed quantities occurred in the first 30 min of the process

time, indicating that the algal biomass is an effective bioadsorbent. It is clear from Figure 4b that the removal efficiency, η , increases with time until it approaches a maximum value. This maximum value decreases as the initial concentration increases. For example, the value of removal efficiency was 76.0%, 49.1%, and 35.0% corresponding to initial concentrations of 50, 100, and 150 mg/L, respectively. This indicates that the algal biomass is more efficient as a desorbing agent in dilute solutions rather than concentrated solutions. It should be noted that as the concentration increases the driving force for the adsorption increases and this leads to an increasing adsorption rate. However, the relative quantity adsorbed decreases as the adsorbate concentration increases.

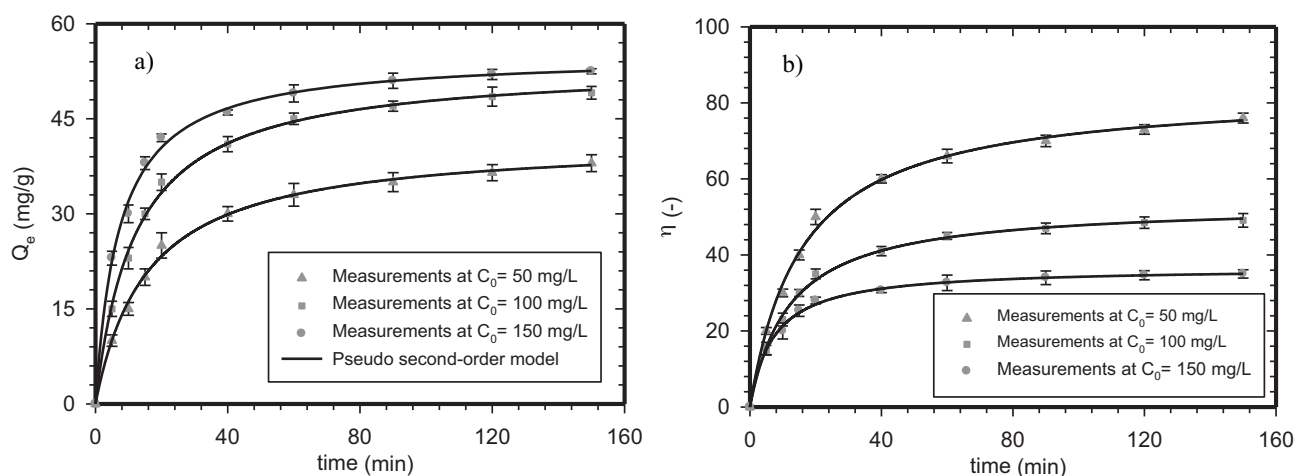


Figure 4. Variations of: a) the adsorption capacity, Q_t , and b) the removal efficiency with time at different initial concentrations using adsorbent mass of 1 g with 300 μm diameter, mixing speed of 150 rpm, pH of 6, and temperature of 30 $^{\circ}\text{C}$.

On the other hand, it is clear from Figure 4a that the data fit the pseudo second-order model well independently of the initial concentration. Values of the model parameters at the operational conditions of 30 $^{\circ}\text{C}$, mixing speed of 300 rpm, and pH of 6 are shown in Table 3. The experimental and model-predicted values of Q_e are also given in Table 3. The value of the kinetic parameter k increases from 7.028 to 15.440 g/(mg h) as the concentration increases from 50 to 240 mg/L with R^2 values close to unity. On the other hand, Table 3 shows that the model slightly overestimates the equilibrium loading capacity of the algal biomass by about 4% to 5%.

Table 3. Pseudo second-order model parameters for different initial Cu^{+2} concentrations at 30 $^{\circ}\text{C}$, mixing speed of 300 rpm, pH of 6, and adsorbent mass of 1 g with diameter of 300 μm .

Initial Cu^{+2} concentration (mg/L)	$q_{e \text{ exp}}$ (mg/g)	Pseudo second-order kinetic model			
		$q_{e \text{ prel.}}$ (mg/g)	k (g/mg h)	R^2	SSE (%)
50	38.5	40.65	7.0276	0.9912	1.22
100	49.1	51.81	7.568	0.9955	1.23
150	52.5	54.94	10.76	0.9985	1.55
180	55	56.18	10.92	0.9983	1.76
240	57.5	58.48	15.48	0.9985	1.72

2.3.2. Effect of solution initial pH on adsorption kinetics

The pH of the ion aqueous solution is considered as a major parameter that controls the adsorption process. In the present study, experiments were conducted for pH values in the range of 3–6. This pH range was chosen to avoid precipitation of Cu^{+2} ions as $\text{Cu}(\text{OH})_2$ above a pH of 6. This range was confirmed by the Cu^{+2} speciation diagram reported by previous studies.^{42,46} They showed graphically that free Cu^{+2} ions represent the dominant species of copper at a pH of ≤ 6 . In addition, the Cu^{+2} ion species is mainly involved in the adsorption process.^{28,47} The effects of pH on the equilibrium loading capacity, Q_e , and the removal efficiency as functions of time are shown in Figure 5. It is evident from Figure 5a that Q_e values are 24.0, 34.5, and 49.1 mg/g corresponding to pH values of 3.5, 4.5, and 6, respectively. In acidic media of pH lower than 6, competition occurs between H_3O^+ and Cu^{+2} ions for the adsorption sites.

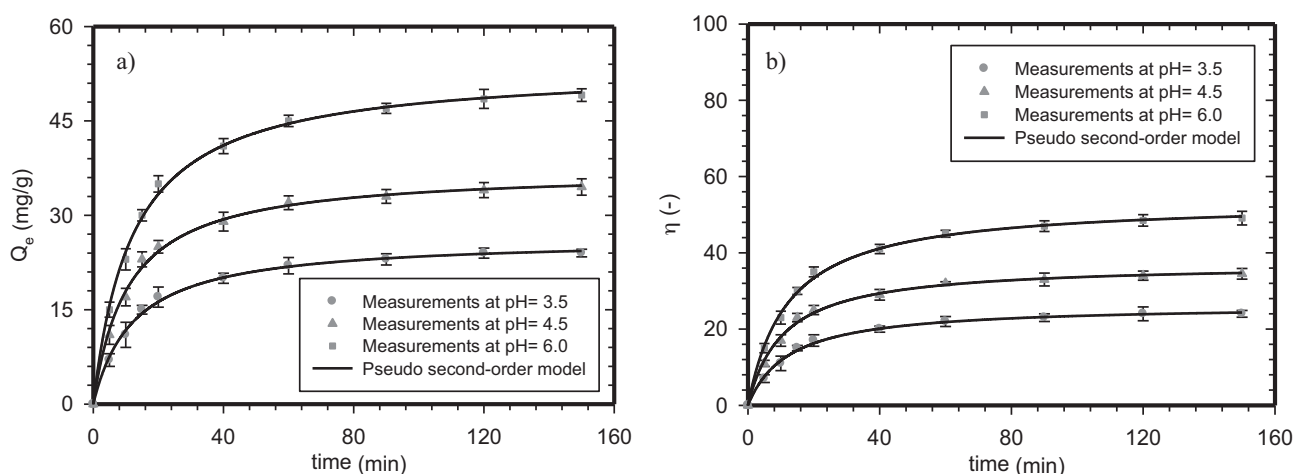


Figure 5. Variations of: a) the adsorption capacity, Q_t , and b) the removal efficiency with time at different pH values using adsorbent mass of 1 g with 300 μm diameter, mixing speed of 150 rpm, C_o of 100 mg/L, and temperature of 30 °C.

Referring to Eq. (1), it was shown that when pH values were in the range of 4.5–6.0, the adsorbent surface charge was mainly negative. On the other hand, the pH range of 4.0 to 4.5 could be called the isoelectric point or the zero charge point since the adsorbent surface has zero net charge. Additionally, the adsorbent surface acquires a net positive charge at pH values below 4. Accordingly, when the solution pH is 5, which is higher than the isoelectric point, the algal biomass acts as a negative surface and attracts the Cu^{+2} ions. Figure 5b shows that the removal efficiency increases with time until it approaches a maximum value. However, this maximum value increases with increasing pH value. For example, the value of the removal efficiency was 24.0%, 34.5%, and 49.1% corresponding to pH values of 3.5, 4.5, and 6.0, respectively. This indicates that the algal biomass is more efficient as an adsorbent agent in weak acidic to neutral solutions. Again, Figure 6 shows that the data fit the pseudo second-order kinetic model well regardless of solution pH value. This ensures that the bioadsorption of Cu^{+2} ions onto algal biomass is described adequately by the pseudo second-order reaction.

2.3.3. Effect of adsorbent dose on adsorption kinetics

Adsorbent dose is an important parameter that controls the adsorbent loading capacity, Q_e . The variations of the adsorption capacity and removal efficiency with time at different adsorbent doses are shown Figure 6. It

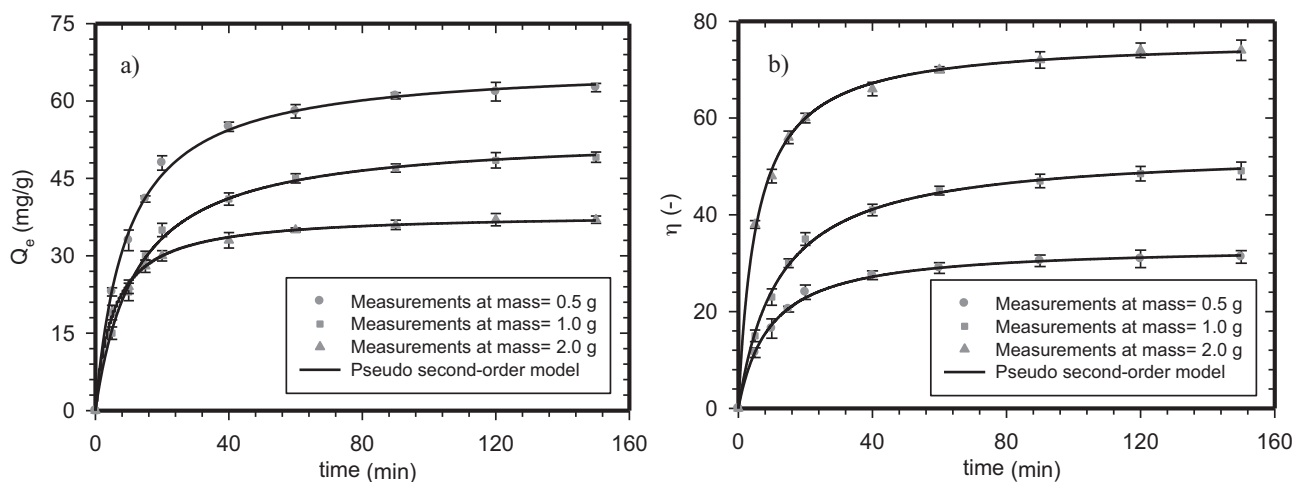


Figure 6. Variations of: a) the adsorption capacity, Q_t , and b) the removal efficiency with time at different adsorbent doses of 300 μm in diameter with mixing speed of 150 rpm, C_0 of 100 mg/L, pH of 6, and temperature of 30 $^\circ\text{C}$.

is evident from Figure 6a that as the algal biomass dose increases from 0.5 to 2.0 g, the equilibrium loading capacity, Q_e , decreases from 62.6 to 37.0 mg/g. On the other hand, the amount adsorbed per unit mass of the adsorbent decreases considerably. This decrease is attributed to the increase in the active sites with increasing adsorbent dose while maintaining the adsorbate concentration constant. This means that as the adsorbent dose increases, more adsorbent-free sites will be available for adsorption and/or chelation.¹¹

Figure 6b shows the variation of removal efficiency, η , with time at different adsorbent doses. It is evident from Figure 6b that η increases with time until it approaches a maximum value. Moreover, this maximum value increases as the adsorbent dose increases. For example, the value of the maximum removal efficiency was 31.1%, 49.1%, and 74.0% corresponding to adsorbent doses of 0.5, 1.0, and 2.0 g, respectively. This indicates that the algal biomass is more efficient at higher adsorbent doses.

2.4. Adsorption thermodynamics

The adsorption isotherm results showed that the equilibrium adsorption capacity, Q_e , of the algal biomass slightly increases as the temperature increases. For example, Q_e increases from 62.5 to 64.5 mg/g as the temperature increases from 30 to 50 $^\circ\text{C}$. This result confirms the endothermic nature of the adsorption of Cu^{+2} ions onto the algal biomass. This behavior is attributed to the effect of temperature on the pore size, liquid phase viscosity, and ions' kinetic energy, as mentioned above.

Eqs. (13) through (15) were used to calculate the thermodynamic parameters for the adsorption process. The effect of temperature on the distribution coefficient, K_d , for different Cu^{+2} ion initial concentrations of 16 to 240 mg/L is shown in Figure 7. As shown in the figure, the relationship between $\ln K_d$ and $1/T$ is linear with square correlation coefficient, R^2 , of about 0.99. In addition, K_d values increase as the temperature increases. However, the values of K_d decrease as the initial concentration increases. This behavior confirms the feasibility of the adsorption process if a low Cu^{+2} ion initial concentration is used.

Table 4 shows the values of the thermodynamic parameters for Cu^{+2} ions' adsorption onto the algal biomass at different initial concentrations with temperatures from 30 to 50 $^\circ\text{C}$. Table 4 shows positive values for both the standard enthalpy of the adsorption process, ΔH° , and the standard entropy of activation, ΔS° . These results confirm the previous isotherm experiments at different temperatures. The positive values of

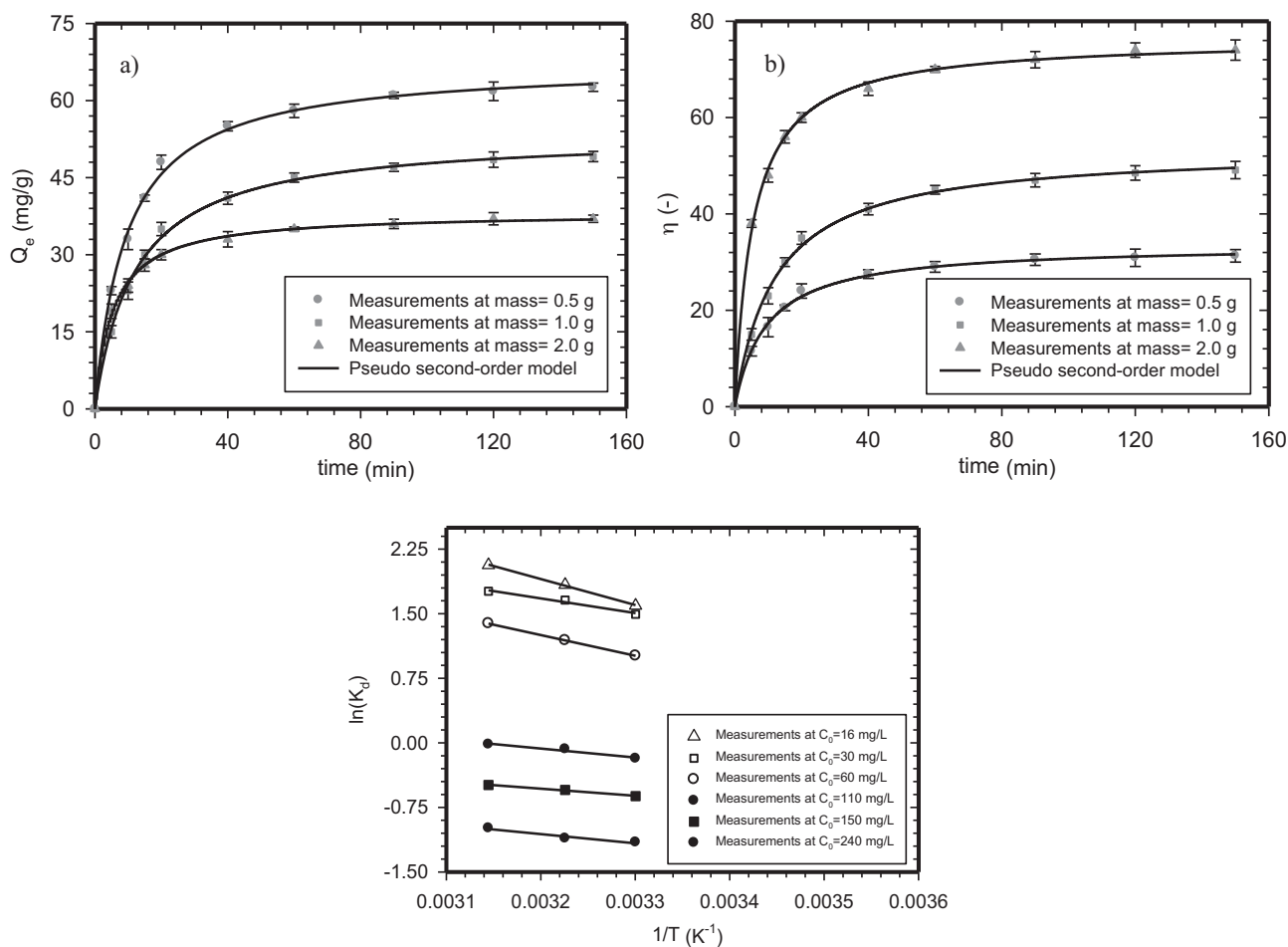


Figure 7. The effect of temperature on the distribution coefficient, K_d , for different initial Cu^{+2} ion concentrations at adsorbent mass 1 g and with $300 \mu\text{m}$ diameter, mixing speed of 150 rpm, and pH of 6.

Table 4. Values of the thermodynamic parameters for Cu^{+2} ions' adsorption onto algal biomass at different initial concentrations at 30°C , mixing speed of 300 rpm, pH of 6, and adsorbent mass of 1 g with diameter of $300 \mu\text{m}$.

Initial concentration (mg/L)	ΔH° (J/mol)	ΔS° (J/mol K)	ΔG° (J/mol)			R^2
			303 K	313 K	323 K	
16	25,126.6	96.2	-4016.8	-4732.5	-5460.8	0.9974
30	14,207.8	59.4	-3763.4	-4273.8	-4655.8	0.9956
60	20,011.8	74.4	-2548.4	-3065.9	-3665.2	0.999
110	8713.07	27.3	459.3	187.5	48.1	0.9915
150	6899.6	17.6	1559.4	1408.6	1294.3	0.9913
240	8839.4	19.5	2909.5	-2860.2	2618.5	0.9653

standard entropy of activation, ΔS° , indicate the affinity of the algal biomass for metal ion adsorbates such as Cu^{+2} ions. On the other hand, the values of the standard Gibbs free energy, ΔG° , were negative at low adsorbate concentrations up to 60 mg/L, indicating a spontaneous process. At higher Cu^{+2} ion concentrations, ΔG° values become positive. Similar observations were reported for the adsorption of methylene blue onto

oil palm fiber-activated carbon and diatomite.⁴⁸ This behavior is attributed to the increased randomness at the interface between the solid liquid phases. However, as is clear in Table 4, the value of ΔS° decreases as the initial concentration increases. These results could represent a strategy for the optimum conditions for adsorption of heavy metals such as Cu^{+2} ions onto algal biomass. This leads to obtaining a better performance if the ion concentration is relatively low and the medium temperature is relatively high.

2.5. Desorption experiments

In the present research, desorption experiments were conducted for two reasons: to examine the tendency of the adsorbent to be regenerated after being exhausted and to test the stability of the interaction between the adsorbate ion and the bioadsorbent surface. The percent desorption by 0.1 M H_2SO_4 and 0.2 M HCl was 94% and 86%, respectively, when the solid bioadsorbent mass-to-liquid volume ratio, S/L, was 100 g/L. Furthermore, the process concentration ratio, CR, defined as the ratio of Cu^{+2} concentration in the desorption solution to the Cu^{+2} concentration initially used in the adsorption process, was evaluated. This parameter could be considered as an efficiency indicator for the bioadsorption process as a whole.⁴⁹ It was found that the CR value was 0.49 and 0.44 for 0.1 M H_2SO_4 and 0.2 M HCl, respectively. Based on these values and on the cost of the desorption solutions, 0.1 M H_2SO_4 solution is a promising desorption agent and it is recommended for the Cu^{+2} desorption process.

Table 5 shows a comparison of the maximum capacity of several adsorbents used to adsorb copper ions. This comparison includes the use of crude and modified algae such as red, green, and brown in addition to active carbon and fungi. It is evident from Table 5 that dead phosphorylated algal biomass of *Spirogyra* has a relatively high adsorption capacity compared to that of activated carbon. Accordingly, modification of green algae by phosphorylation is a promising chemical process to produce a cheap and effective adsorbent.

Table 5. A comparison of various bioadsorbents used to adsorb copper ions.

Bioadsorbent	Maximum capacity, mg/g	Reference
Red algae (<i>Palmaria palmata</i>)	12.7	50
Brown algae, <i>Fucus vesiculosus</i>	60.5	37
Dead biomass, <i>Spirogyra</i> species	34.94	7
Brown algae	50.4	51
Green algae	47.2	52
Red algae	40.3	53
Fungus	20.79	53
Modified algae	143	38
Activated carbon	63	54
Modified algae	65	Present study

3. Experimental

3.1. Preparation and characterization of biomass

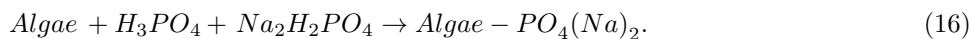
Samples of *Spirogyra*, a common filamentous green algal biomass, were collected from a fresh water pool used for crop irrigation (Alrsaifah, Jordan). These green algae are usually available in abundance in such pools. After sample collection, it was thoroughly washed with tap water to remove dirt and other unwanted material, and then washed with distilled water. The sample then was squeezed and water was decanted. The sample was dried at 90 °C for 6 h in a drying oven to remove moisture. After that the biomass sample was ground using

a mortar. The ground sample was sieved for several fractions. The particles with diameters of 300 μm were selected.

To characterize the surface and pore properties of the algae, scanning electron microscopy (SEM) was used. EDS analysis was performed to determine the elemental and weight ratios in algal biomass samples. The SEM and EDS device was the model SUPERSCAN SSX-550, Shimadzu. Infrared spectra of the algae were analyzed using FT-IR spectroscopy with the model 8400S, Shimadzu. FT-IR spectra were recorded in the range of 4000–400 cm^{-1} using 2 mg of the sample mixed with 200 mg of KBr (FT-IR grade) pressed into a pellet. The pellet was immediately put into the sample holder.

3.2. Phosphorylation of green algae

The aim of phosphorylation was to introduce new active sites capable of reacting with heavy metals to increase the adsorption capacity. A sample of the dried and ground green algae previously prepared was used in this phosphorylation step and 4.0 g of green algae sample was mixed with 5.0 g of urea and 5.0 g of phosphate. Phosphate consisted of 2.0 g of phosphoric acid and 3.0 g of monosodium phosphate. The mixture was then shaken in a thermostated shaker (Gallenkamp, UK) at 30 $^{\circ}\text{C}$ for 35 min. After that, the mixture was placed in a drying oven at 70 $^{\circ}\text{C}$ for 60 min. The biomass was then mixed with 100 mL of dimethyl formamide and put into a muffle furnace for 5 h at 100 $^{\circ}\text{C}$ to complete the reaction. The reaction can be expressed by the following equation:



The expected reaction with a divalent heavy metal such as Cu^{+2} could be expressed as:



Finally, the phosphorylated biomass was cooled, separated from the solution by centrifugation, and washed with distilled water to remove any excess of unreacted reagents. The phosphorylated algae were then characterized using FT-IR and EDS instruments.

3.3. Preparation of copper(II) solution

Copper(II) stock solutions were prepared by dissolving an accurate weight of $\text{CuSO}_4 \cdot 5\text{H}_2\text{O}$ in distilled water. The initial pH of each solution was adjusted to 3.5, 4.5, and 6.0 with 1.0 M HCl and NaOH solutions. Spectrophotometric analysis was done at a wavelength of 580 nm using a Jenway PCO1 spectrophotometer. A standard calibration curve (figure not shown) of Cu^{+2} solution was constructed with a squared correlation coefficient (R^2) value close to 0.9978, which reflects a high correlation in the study's targeted Cu^{+2} concentration range.

3.4. Adsorption isotherms

Adsorption isotherm experiments of Cu^{+2} ions by algae were conducted by suspending 0.500 to 2.00 g of dry ground algae in 100 mL of Cu^{+2} solutions in glass bottles with screw caps. The initial Cu^{+2} concentrations ranged from 40 to 400 ppm. An orbital shaker bath operated at 150 rpm was used to shake the suspensions and to maintain them at constant temperature for 24 h. After this period, the bioadsorption process was assumed to have reached equilibrium conditions. The suspensions were then centrifuged and the filtrate was analyzed to get the Cu^{+2} concentration using atomic absorption spectroscopy. This procedure was repeated for three different temperatures of 30, 40, and 50 $^{\circ}\text{C}$ at pH 6 and for three pH values of 3.5, 4.5, and 6 at 30 $^{\circ}\text{C}$.

In this part of the study, the amount of Cu^{+2} ions adsorbed by algae at equilibrium, Q_e , mg Cu^{+2} per g adsorbent, was calculated according to the following mass balance equation:

$$Q_e = \frac{(C_o - C_e)V}{W}, \quad (18)$$

where V is the solution volume in L and W is the adsorbent mass in g.

3.5. The kinetic study

The kinetic study experiments were performed using a batch technique in 100-mL Erlenmeyer flasks. A thermostated shaker was used to induce mixing and to ensure isothermal conditions over the period of each experiment with ± 1 °C accuracy. Samples of Cu^{+2} solutions were continuously withdrawn from the flask at certain time intervals using a suitable syringe and then centrifuged at 5000 rpm for 10 min using a Hettich centrifuge. All kinetic experiments continued until equilibrium conditions were assumed to be reached when the Cu^{+2} concentration took a near constant value. The effect of initial concentration, pH, adsorbent dose, and temperature on the adsorption of Cu^{+2} ions was investigated.

In the kinetics part of the present study, the amount of adsorbed Cu^{+2} was calculated using:

$$Q_t = \frac{(C_o - C_t)V}{W}, \quad (19)$$

where C_o and C_t are Cu^{+2} initial and time function concentration in mg/L, respectively.

The data of Cu^{+2} adsorption kinetics onto the algal surface were analyzed using the least square method, in which the sums of squared errors (SSE, %) is given by:⁵⁵

$$SSE = \sqrt{\frac{\sum (Q_{e,\text{exp.}} - Q_{e,\text{cal.}})^2}{N}}, \quad (20)$$

where N is the number of data points. Usually a low SSE value indicates a better fit. Experiments were performed in triplicate while maintaining the experimental conditions to obtain reproducible results with an experimental error of less than 4%. The percent removal efficiency (η) was estimated using:

$$\eta = \frac{C_o - C_e}{C_o} \times 100\%. \quad (21)$$

3.6. Desorption experiments

Desorption experiments were conducted to examine the ease of metal ion–algal cells disengagement and separation for possible recycling and reuse.⁵⁶ In these experiments, 1.0 g of the algae was first contacted for 10 h with a 50 mg/L solution of Cu^{+2} ions. The mixture was then filtered and put into an oven for 24 h to dry at 60 °C. One gram of the dried and exhausted biomass was then contacted with 50 mL of the desorbing agent solution for 150 min and 50 rpm. The desorbing agents used were H_2SO_4 and HCl. Solutions of these two acids were prepared in different concentrations of 0.001, 0.01, and 0.1 M using deionized water. A relatively high value of solid bioadsorbent mass-to-liquid volume ratio, S/L, of 100 g/L was used to produce highly concentrated Cu^{+2} ion solution. All experiments were done in triplicate.

The present research was conducted to modify the structure of dead green algae cells by phosphorylation and to assess the optimum operating parameters for the adsorption of Cu^{+2} ions onto the phosphorylated green algal biomass. Phosphorylation as a chemical surface modification reaction was found to increase the phosphorus content of the biomass fivefold. The increased phosphate content increases the adsorption capacity by about 50% compared to raw or unphosphorylated cells. Green algal biomass was found to be a cheap and effective bioadsorbent for heavy metal ions such as Cu^{+2} . The Langmuir adsorption isotherm model was found to fit the experimental isotherm data better than the Freundlich model, indicating a monolayer formation of Cu^{+2} ions on the algal surface. The maximum adsorption capacity of the algal biomass was found to increase as the temperature increased, indicating an endothermic process. As the adsorbent dose increases the equilibrium adsorption capacity of the algal biomass decreases, while the removal efficiency of Cu^{+2} ions increases. The optimum pH value was about 6, where the algal biomass acquires a net negative charge. Values of the thermodynamic data revealed that the adsorption process is spontaneous at relatively low Cu^{+2} concentrations accompanied by a net increase in entropy. H_2SO_4 is recommended as an efficient regeneration agent of the algal biomass that removes more than 96% of the adsorbed Cu^{+2} ions. The obtained results from the present research are encouraging and give initiative to design a continuous process for heavy metal ions' removal from industrial wastewater treatment by using algae as an efficient and generable bioadsorbent. This continuous process will be the subject of further investigations in our labs.

References

1. Al-Qodah, Z. *Desalination* **2006**, *196*, 164-176.
2. Bani-Melhem, K.; Al-Qodah, Z.; Al-Shannag, M.; Qasaimeh, A.; Qtaishat, M. R.; Alkasrawi, M. *J. Membrane Sci.* **2015**, *476*, 40-49.
3. Al Momani, F.; Shawaqfah, M.; Shawaqfeh, A.; Al-Shannag, M. *J. Environ. Sci.* **2008**, *20*, 675-682.
4. Mukhopadhyay, M.; Noronha, S. B.; Suriaishkumar, G. K. *Bioresour. Technol.* **2007**, *98*, 1781-1787.
5. Al-Rub, F. A. A.; El-Naas, M. H.; Ashour, I.; Al-Marzouqi, M. *Process Biochem.* **2006**, *41*, 457-464.
6. Ghodbane, I.; Nouri, L.; Hamdaoui, O.; Chiha, M. *J. Hazard. Mater.* **2008**, *152*, 148-158.
7. Bishnoi, N. R.; Pant, A.; Garima, P. *J. Sci. Ind. Res.* **2004**, *113*, 813-816.
8. Lakshmi, K. B.; Sudha, P. N. *Int. J. Environ. Sci.* **2012**, *3*, 453-470.
9. Brauckmann, B. M. *Biosorption*; CRC Press: Boca Raton, FL, USA, 1990.
10. Al-Shannag, M.; Al-Qodah, Z.; Bani-Melhem, K.; Qtaishat, M. R.; Alkasrawi, M. *Chem. Eng. J.* **2015**, *260*, 749-756.
11. Zalloum, H. M.; Al-Qodah, Z.; Mubarak, M. S. *J. Macromol. Sci. A* **2009**, *46*, 46-57.
12. Kandah, M.; Al-Rub, F. A. A.; Al-Dabaybeh, N. *Adsorpt. Sci. Technol.* **2003**, *21*, 501-509.
13. Gong, R.; Guan, R.; Zhao, J.; Liu, X.; Ni, S. *J. Health Sci.* **2008**, *54*, 174-178.
14. Şengil, İ. A.; Özacar, M. *J. Hazard. Mater.* **2008**, *157*, 277-285.
15. Siao, P. C.; Li, G. C.; Engle, H. L.; Iiao, L. V.; Trinidad, L. C. *J. Appl. Phycol.* **2007**, *19*, 733-743.
16. Ahmad, A.; Rafatullah, M.; Sulaiman, O.; Ibrahim, M. H.; Chii, Y. Y.; Siddique, B. M. *Desalination* **2009**, *247*, 636-646.
17. Yazıcı, H.; Kılıç, M.; Solak, M. *J. Hazard. Mater.* **2008**, *151*, 669-675.
18. Šćiban, M.; Klačnjak, M.; Škrbić, B. *Desalination* **2008**, *229*, 170-180.
19. Chen, H.; Dai, G.; Zhao, J.; Zhong, A.; Wu, J.; Yan, H. *J. Hazard. Mater.* **2010**, *177*, 228-236.

20. Al-Qodah, Z.; Shawaqfeh, A.; Lafi, W. *Adsorption* **2007**, *13*, 73-82.
21. Al-Qodah, Z.; Lafi, W. *J. Water Supply Res. T.* **2003**, *52*, 189-198.
22. Al-Qodah, Z. *J. Eng. Technol* **1998**, *17*, 128-137.
23. Yahya, M. A.; Al-Qodah, Z.; Ngah, C. Z. *Renew. Sustainable Energy Rev.* **2015**, *46*, 218-235.
24. Bailey, S. E.; Olin, T. J.; Bricka, R. M.; Adrian, D. D. *Water Res.* **1999**, *33*, 2469-2479.
25. Low, K. S.; Lee, C. K.; Liew, S. C. *Process Biochem.* **2000**, *36*, 59-64.
26. Lodi, A.; Solisio, C.; Converti, A.; Del Borghi, M. *Bioprocess. Eng.* **1998**, *19*, 197-203.
27. Karthika, T.; Thirunavukkarasu, A.; Ramesh, S. *Recent Research in Science and Technology* **2010**, *2*, 86-91.
28. Demirbas, E.; Dizge, N.; Sulak, M. T.; Kobya, M. *Chem. Eng. J.* **2009**, *148*, 480-487.
29. Yan, G.; Viraraghavan, T. *Water SA* **2000**, *26*, 119-124.
30. Gong, R.; Ding, Y.; Liu, H.; Chen, Q.; Liu, Z. *Chemosphere* **2005**, *58*, 125-130.
31. Dilek, F. B.; Gokcay, C. F.; Yetis, U. *Water Res.* **1998**, *32*, 303-312.
32. Rajfur, M. *Ecol. Chem. Eng. S.* **2013**, *20*, 23-40.
33. Sweetly, J. *Int. J. Pharm. Biol. Sci. Arch.* **2014**, *5*, 17-26.
34. Brinza, L.; Dring, M. J.; Gavrilesco, M. *Environ. Eng. Manag. J.* **2007**, *6*, 237-251.
35. Hassan Khani, M.; Reza Keshtkar, A.; Meysami, B.; Firouz Zarea, M.; Jalali, R. *Electron. J. Biotechn.* **2006**, *9*, 100-106.
36. Parameswari, E.; Lakshmanan, A.; Thilagavathi, T. *J Algal Biomass Util.* **2009**, *1*, 9-17.
37. Ahmady-Asbchin, S.; Mohammadi, M. *J. Biol. Environ. Sci* **2011**, *5*, 121-127.
38. Mikati, F. M.; Saade, N. A.; Slim, K. A.; El Jamal, M. M. *J. Chem. Technol. Metall.* **2013**, *48*, 61-71.
39. Soleymani, F.; Pahlevanzadeh, H.; Khani, M. H.; Manteghian, M. *Iran. J. Chem. Eng.* **2014**, *11*, 57.
40. Vilar, V. J. P.; Botelho, C. M. S.; Pinheiro, J. P. S.; Domingos, R. F.; Boaventura, R. A. R. *J. Hazard. Mater.* **2009**, *163*, 1113-1122.
41. Weber, T. W.; Chakravorti, R. K. *AIChE J.* **1974**, *20*, 228-238.
42. Kannan, S. *Int. J. Curr. Microbiol. App. Sci* **2014**, *3*, 341-351.
43. Ho, Y. S. *J. Hazard. Mater.* **2006**, *136*, 681-689.
44. Gupta, V. K.; Ali, I. *Water Res.* **2001**, *35*, 33-40.
45. Sakairi, N.; Shirai, A.; Miyazaki, S.; Tashiro, H.; Tsuji, Y.; Kawahara, H.; Yoshida, T.; Nishi, N.; Tokura, S. *Jpn. J. Polymer. Sci. Technol.* **1998**, *55*, 212-216.
46. Wang, X. S.; Qin, Y. *Process Biochem.* **2005**, *40*, 677-680.
47. Al-Qodah, Z.; Lafi, W.; Al-Anber, Z.; Al-Shannag, M.; Harahsheh, A. *Desalination* **2007**, *217*, 212-224.
48. Ahamed, J. A.; Begum, A. S. *Arch. Appl. Sci. Res* **2012**, *4*, 1532-1539.
49. Atkinson, B. W.; Bux, F.; Kusan, H. C. *Water SA* **1998**, *24*, 129-135.
50. Li, Y.; Helmreich, B.; Horn, H. *Materials Sciences and Applications* **2011**, *2*, 70-80.
51. Davis, T. A.; Volesky, B.; Mucci, A. *Water Res.* **2003**, *37*, 4311-4330.
52. Sheng, P. X.; Ting, Y. P.; Chen, J. P.; Hong, L. *J. Colloid Interface Sci.* **2004**, *275*, 131-141.
53. Romera, E.; Gonzalez, F.; Ballester, A.; Blazquez, M.; Munoz, J. *Bioresour. Technol.* **2008**, *99*, 4684-4693.
54. Balakrishnan, V.; Arivoli, S.; Begum, A.; Ahamed, A. *J. Chem. Pharm. Res.* **2010**, *2*, 176-190.
55. Al-Shawbkah, R.; Al-Qodah, Z.; Al-Bsoul, A. *Desalin. Water Treat.* **2015**, *53*, 2555-2564.
56. Al-Qodah, Z.; Al-Shannag, M.; Amro, A.; Assirey, E., BoB, M.; Bani Melhem, K.; Al-Kasrawi, M. *Desalin. Water Treat.* (In Press).